

Control of particle clustering in turbulence by polymer additives

F. De Lillo,^{1,2} G. Boffetta,^{1,2} and S. Musacchio^{3,2}

¹*Department of Physics and INFN, University of Torino, via P. Giuria 1, 10125 Torino, Italy*

²*International Collaboration on Turbulence Research*

³*CNRS, Laboratoire J.A. Dieudonné UMR 6621 - Parc Valrose, 06108 Nice, France, EU*

We study the clustering properties of inertial particles in a turbulent viscoelastic fluid. The investigation is carried out by means of direct numerical simulations of turbulence in the Oldroyd-B model. The effects of polymers on the small scale properties of homogeneous turbulence are considered in relation with their consequences on clustering of particles, both lighter and heavier than the carrying fluid. We show that, depending on particle and flow parameters, polymers can either increase or decrease clustering.

Clustering of inertial particles in turbulent flows is relevant for meteorology and engineering, as well as fundamental research. It is believed to play a crucial role in rain-drop formation [1], as well as in the aggregation of proto-planetesimals in Keplerian accretion disks [2]. The physical mechanism which originates such clustering is indeed rather simple: particles heavier than the fluid in which they are transported experience inertial forces which expel them from vortices; particles lighter than the fluid are attracted into vortical structures, for similar reasons [3–5]. In realistic flows, however, particles are advected by the small scale vortical structures of turbulent flows: these have highly non-trivial statistical features, resulting in a complex clustering process which is still far from being completely understood. From the point of view of applications, the properties of concentration and distribution of inertial particles play a crucial role in engineering and for the design of industrial processes involving combustion and mixing [6–8]. Suspensions of particles in viscoelastic fluids are used in many products of commercial and industrial relevance [9].

In this paper we investigate, by means of direct numerical simulations of a turbulent flow, how the clustering properties of a dilute suspension of inertial particles can be affected by the addition of small amounts of polymer additives. The effects induced by polymers on turbulent flows are themselves of enormous relevance. It is enough to mention the celebrated drag reduction effect which occurs in pipe flows [10], or the recently discovered elastic turbulence regime [11]. Polymers have striking effects also on Lagrangian properties of the flow. In particular it has been shown that polymer addition in turbulent flows reduces the chaoticity of Lagrangian trajectories [12] and affects acceleration of fluid tracers [13]. Conversely in the elastic turbulence regime polymers are able to generate Lagrangian chaos in flows at vanishing Reynolds number, which would be non chaotic in the Newtonian case [12, 14].

Here we show that the addition of polymers in a turbulent flow has important effects on the statistical properties of inertial particles which can result in both an increase or a decrease of the clustering. An example of the effect of polymers on clustering is shown in Fig. 1 which represents the distribution of an ensemble of inertial par-

ticles in a turbulent flow before and after the introduction of polymers. It is evident, already at the qualitative level of Fig. 1, that polymers are able to change the statistical distribution of particles. We show that these effects can be understood and quantified in terms of the Lyapunov exponents of inertial particles, which are very sensitive to the presence of polymers. Previous systematic investigations of inertial particle dynamics in Newtonian turbulent flows [15] and stochastic flows [16] have shown that clustering (quantified by means of the Lyapunov Dimension of particle attractor) is maximum when the particle relaxation time is of the order of the shortest characteristic time of the flow.

We consider the case of a dilute suspension of small inertial particles, in which the effects of the disturbance flow induced by the particles can be neglected. The dynamics of the suspension is hence modeled by an ensemble of non-interacting point particles, which experience viscous drag and added mass forces. The equation of motion of each particle reads [18]:

$$\frac{d\mathbf{x}}{dt} = \mathbf{v} \quad (1)$$

$$\frac{d\mathbf{v}}{dt} = -\frac{1}{\tau_S} [\mathbf{v} - \mathbf{u}(\mathbf{x}(t), t)] + \beta \frac{d\mathbf{u}}{dt} \quad (2)$$

where $\tau_S = a^2/(3\beta\nu)$ is the Stokes relaxation time, a is the particle radius, $\beta = 3\rho_f/(\rho_f + 2\rho_p)$ (ρ_p and ρ_f representing particle and fluid densities respectively) and ν is the kinematic viscosity of the fluid (replaced by the total viscosity ν_T in a viscoelastic fluid, see below). Light (heavy) particles correspond to $\beta > 1$ ($\beta < 1$). In this work we consider the two extreme cases of very light particles (e.g. air bubble in water) for which $\beta = 3$ and very heavy particles with $\beta = 0$. We define the Stokes number as $St = \tau_S \lambda_1^0$, where λ_1^0 is the maximum Lyapunov exponent of neutral Lagrangian tracers (i.e. $St = 0$ particles) in the flow. With this definition, maximum clustering is obtained for $St \simeq 0.1$ [15, 16].

The viscoelastic flow $\mathbf{u}(\mathbf{x}, t)$ in which the particles are suspended can be described by standard viscoelastic models, such as the Oldroyd-B model or the nonlinear FENE-P model, which accounts for the finite extensibility of polymers. In spite of their simplicity, these models are able to reproduce many relevant properties of

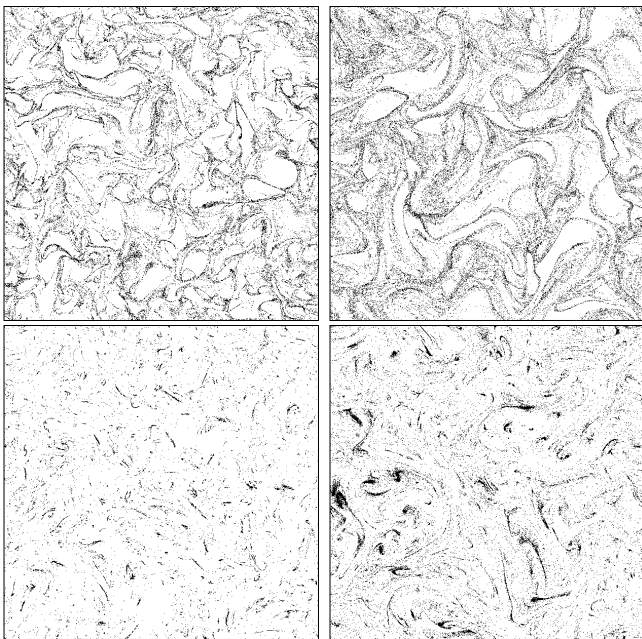


FIG. 1: Section on plane $z = 0$ of the distribution of heavy particles with $\tau_S = 0.035$ (upper panels) and light particles with $\tau_S = 0.03$ (lower panels) in statistically stationary conditions in a Newtonian flow (left) and a viscoelastic flow at $Wi = 1$ (right). Both flows are forced with the same forcing $\mathbf{f}(\mathbf{x}, t)$ δ -correlated in time and localized on large scales. Numerical simulations are done by a pseudo-spectral, fully dealiased code at resolution 256^3 . For the viscoelastic simulations, a small diffusive term is added to (4) to prevent numerical instabilities [17].

dilute polymer solutions, including turbulent drag reduction [19, 20] and elastic turbulence phenomenology [21]. Here we choose the Oldroyd-B model [22], in which the coupled dynamics of the velocity field $\mathbf{u}(\mathbf{x}, t)$ and the polymer conformation tensor $\sigma(\mathbf{x}, t)$ (which is proportional to local square polymer elongation) reads:

$$\frac{\partial \mathbf{u}}{\partial t} + \mathbf{u} \cdot \nabla \mathbf{u} = -\nabla p + \nu \nabla^2 \mathbf{u} + \frac{2\nu\gamma}{\tau_p} \nabla \cdot \sigma + \mathbf{f} \quad (3)$$

$$\frac{\partial \sigma}{\partial t} + \mathbf{u} \cdot \nabla \sigma = (\nabla \mathbf{u})^T \cdot \sigma + \sigma \cdot (\nabla \mathbf{u}) - \frac{2}{\tau_p} (\sigma - \mathbb{I}) \quad (4)$$

The total viscosity of the solution $\nu_T = \nu(1 + \gamma)$ is written in terms of the kinematic viscosity of the solvent ν and the zero-shear contribution of the polymer γ which is proportional to the polymer concentration. The polymer time τ_p represents the longest relaxation time to the equilibrium configuration ($\sigma = \mathbb{I}$ in dimensionless units). Viscoelasticity of the turbulent flow is parametrized by the Weissenberg number Wi , the ratio between τ_p and a characteristic time of the flow. Here we use $Wi = \tau_p \lambda_1^N$ where λ_1^N is the Lagrangian Lyapunov exponent of the Newtonian flow, before the addition of polymers (i.e. (3) with $\gamma = 0$). We stress that λ_1^0 introduced above refers instead to the specific flow that carries the suspension and it clearly depends on Wi . Therefore $\lambda_1^N \equiv \lambda_1^0|_{Wi=0}$.

In the following we discuss results obtained by integrating numerically the viscoelastic model (3-4) at high resolution for different values of Wi (see Table I). The flow is sustained by a stochastic Gaussian forcing $\mathbf{f}(\mathbf{x}, t)$ δ -correlated in time and localized on large scales. Fluid equations were integrated by means of a standard, fully dealiased, pseudo spectral code, on a cubic, triple-periodic domain with 256 grid points per side. When the flow reaches a turbulent, statistically stationary state, different families (i.e. with different values of parameters β and τ_S) of inertial particles are injected, with initial homogeneous distribution in space, and their motion integrated according to (1-2). For each value of Wi , we integrated the motion of 1024 particles for each of 21 values of τ_S and two values of β , namely very heavy particles with $\beta = 0$ and "bubbles" with $\beta = 3$.

As an effect of inertia the distribution of particles does not remain homogeneous and evolves to a fractal set dynamically evolving with the flow, such as the examples shown in Fig. 1. In the language of dynamical systems, the equations (1-2) for particle motion represent a dissipative system whose chaotic trajectories evolve to a fractal attractor (which evolves in time following the flow). A quantitative measure of clustering at small scales is therefore obtained by measuring the fractal dimension of the attractor (for each family of particles) using the Lyapunov dimension [16, 23] defined in terms of Lyapunov exponents as $D_L = K + \sum_{i=1}^K \lambda_i / |\lambda_{K+1}|$ where K is the largest integer for which $\sum_{i=1}^K \lambda_i \geq 0$ [24]. Since the space distribution of the particles is the projection of the attractor on the sub-space of particle positions, the fractal dimension of clusters is given by $\min(D_L, 3)$ [25, 26], provided that the projection is generic (for a discussion on this issue see e.g. [27]). This implies that $D_L < 3$ gives fractal distributions of dimension D_L , while $D_L > 3$ corresponds to space-filling configurations, which however can be non-homogeneous.

In Fig. 2 we plot the fractal dimensions for both heavy and light particles as a function of τ_S for the three simulations at different Wi . It is evident that the addition of polymer changes substantially the clustering properties of the particles, both increasing D_L and reducing D_L depending on value of τ_S . Figure 1 shows examples of clustering reduction, for heavy and light particles respectively. The upper panels refer to heavy particles ($\beta = 0$)

| Wi | ε_f | ε_ν | u_{rms} | λ_1^0 |
|------|-----------------|-------------------|-----------|---------------|
| 0 | 0.28 | 0.28 | 0.76 | 1.36 |
| 0.5 | 0.28 | 0.18 | 0.73 | 1.08 |
| 1 | 0.28 | 0.092 | 0.68 | 0.75 |

TABLE I: Parameters for the Newtonian and viscoelastic simulations. The Weissenberg number Wi , energy input ε_f , viscous dissipation rate ε_ν , rms velocity u_{rms} and Lagrangian Lyapunov exponent λ_1^0 of the carrier flow are shown. In both viscoelastic runs an additional dissipative term was added on polymers (see text), with coefficient $\nu_p = 2.3 \times 10^3$

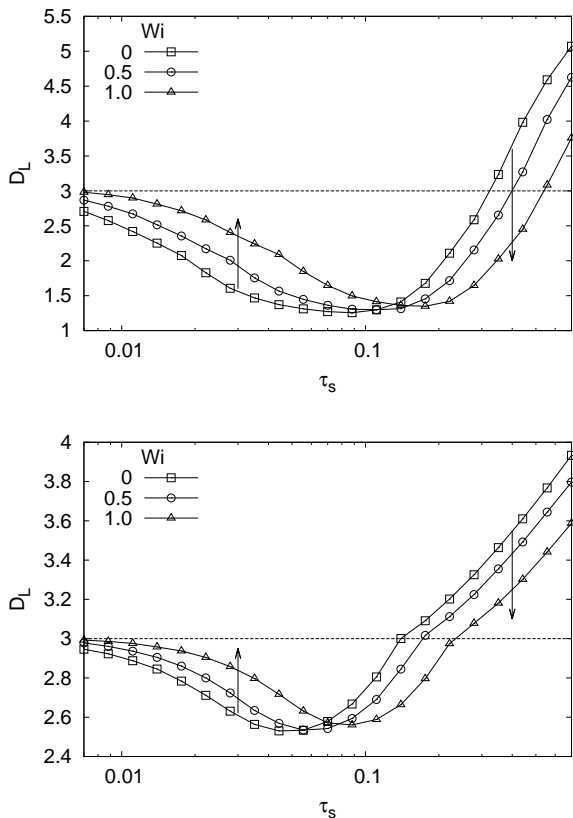


FIG. 2: Lyapunov dimension for light (upper panel) and heavy (lower panel) particles plotted as a function of τ_S . Different lines correspond to the different Weissenberg numbers: $Wi = 0$ (squares), $Wi = 0.5$ (circles) and $Wi = 1.0$ (triangles).

with $\tau_S = 0.035$, while the bottom ones are extracted from a simulation with $\beta = 3$ and $\tau_S = 0.03$. Both values of Stokes time are, for the Newtonian flow, on the left of the minimum in D_L . As a consequence, polymers produce a reduction of clustering. Such effect is more visible for light particles. A possible reason for this difference will be discussed further on.

The mechanism at the basis of this effect is not trivial and is a consequence of the change induced by the polymers on the small-scale properties of the turbulent flow. In Fig.3 we plot the energy spectra for the different Wi numbers. The effect of polymers is evident in the high-wavenumber range where velocity fluctuations are clearly suppressed, resulting in a depletion of the energy spectrum, while large-scale fluctuations are unaffected.

Indeed one can expect that only the fastest eddies of the flow, i.e. those whose eddy turn-over time τ_ℓ is shorter than the polymer relaxation time τ_p , can produce a significant elongation of polymers. The elastic feedback therefore affects only small scales ℓ with $\tau_\ell < \tau_p$. Conversely, large scales exhibit the same phenomenology of a Newtonian flow, characterized by a turbulent cascade with a constant energy flux equal to the energy input rate ε_f . The turbulent cascade proceeds almost unaffected by

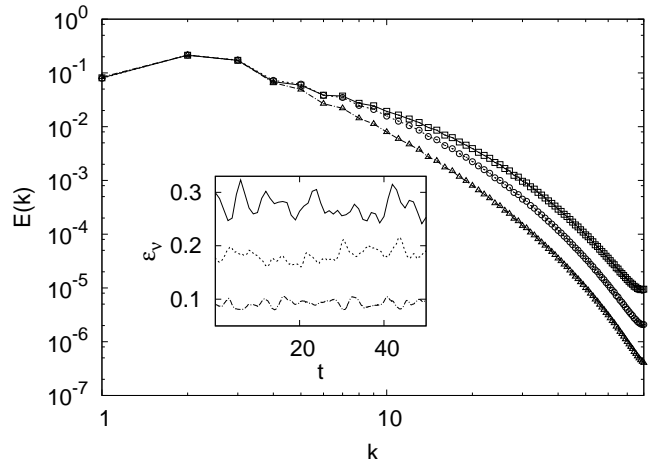


FIG. 3: Energy spectra for the Newtonian case $Wi = 0$ (squares) and for the viscoelastic ones $Wi = 0.5$ (circles) and $Wi = 1$ (triangles). The depletion due to polymer feed-back is evident on large wavenumbers, while the larger scales are unaffected. The effect of polymers extends at lower wavenumbers as Wi increases. Inset: viscous energy dissipation ε_ν during a typical time interval in the stationary simulations, for the Newtonian (solid line), $Wi = 0.5$ (dashed line) and $Wi = 1$ (dash-dot) flows. The decrease in ε_ν with Wi is evident, as well as the reduction in fluctuations.

the presence of polymers down to the Lumley scale ℓ_L , whose eddy turn-over time equals the polymer relaxation time. A dimensional estimate, based on the Kolmogorov scaling for the typical velocity $u_\ell \sim \varepsilon_f^{1/3} \ell^{1/3}$ and turn-over time $\tau_\ell = \ell/u_\ell \sim \varepsilon_f^{-1/3} \ell^{2/3}$ of an eddy of size ℓ , gives $\ell_L = \tau_p^{3/2} \varepsilon_f^{1/2}$. Polymers would therefore affect only the small scales $\ell < \ell_L$. Our results are in qualitative agreement with this picture: the $Wi = 0.5$ spectrum differs from the Newtonian one only for $k \gtrsim 8$, while at $Wi = 1$ polymers are active over a larger range of scales. The reduction of kinetic energy at small scales, due to the transfer of energy to the polymers, is accompanied by a reduction of the viscous dissipation $\varepsilon_\nu = \nu \langle (\nabla u)^2 \rangle$ at fixed energy input ε_f , as can be seen from Table I and in the inset of Fig.3. This phenomenon has been previously observed both in forced and decaying simulations of statistically homogeneous and isotropic turbulence (see, e.g., [28, 29]).

The suppression of small-scale motions caused by polymers has major consequences also on the Lagrangian statistics. It is responsible of the reduction of chaoticity of Lagrangian trajectories [30]. Indeed the chaoticity of the flow is directly related to its stretching efficiency via the Lyapunov exponents. When polymers are stretched, the elastic stress tensor produces a negative feed-back on small scale stretching, thus reducing the degree of chaoticity of the flow [30, 31]. This effect is clearly observable in the decrease of the Lagrangian Lyapunov exponent of the flow at increasing polymer elasticity (see

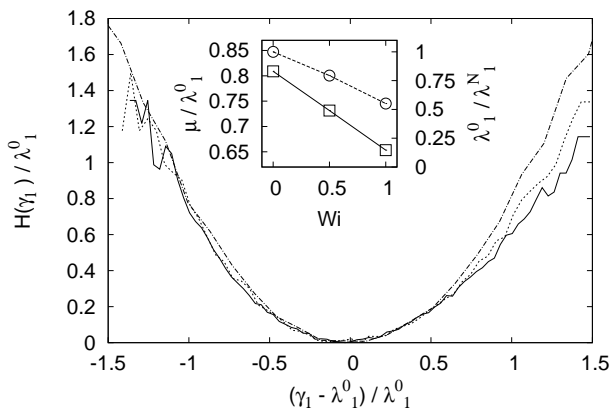


FIG. 4: Comparison between the Cramér functions of the stretching rate γ_1 computed at $Wi = 0$ (solid line), $Wi = 0.5$ (dashed line), $Wi = 1$ (dash-dot). Inset: first Lagrangian Lyapunov exponent λ_1^0 (circles) and width μ (squares) of the Cramér function (see text) as a function of Wi . The Lyapunov exponents are compared with the Newtonian value λ_1^N .

the inset of Fig.4).

It is worth to notice that, because of polymers counteraction, the Lyapunov exponent of the resulting viscoelastic flow is smaller than τ_p^{-1} . In other words, the Wi number computed a posteriori (i.e. after polymer injection) is always smaller than unity. This is not in contrast with the hypothesis that polymers have a strong active effect on the flow mainly when they are stretched, i.e. above the so-called coil-stretch transition, which is expected to happen around $Wi \simeq 1$ [32]. Indeed, the Lyapunov exponent simply provides a measure of the average stretching in a chaotic flow. One should bear in mind that large fluctuations of the stretching rates (and therefore strong viscoelastic effects) can occur also when $Wi \lesssim 1$.

Detailed information on the fluctuations of the stretching rates can be obtained from the statistics of the Finite Time Lyapunov Exponents (FTLE) γ_i . The FTLE are defined via the exponential growth rate during a finite time T of an infinitesimal M -dimensional volume as $\sum_{i=1}^M \gamma_i = (1/T) \ln[V^M(T)/V^M(0)]$ [24]. From the definition of the Lyapunov exponents it follows that $\lim_{T \rightarrow \infty} \gamma_i^T = \lambda_i$. A large deviation approach suggests that the probability density function (PDF) of the largest stretching rate γ_1 measured over a long time $T \gg 1/\lambda_1$ takes the asymptotic form $P_T(\gamma_1) \sim N(t) \exp[-H(\gamma_1)T]$ where the Cramér function $H(\gamma_1)$ is convex and obeys the conditions $H(\lambda_1) = 0$, $H'(\lambda_1) = 0$. We computed the Cramér function for the Lagrangian FTLE for the Newtonian case and the two viscoelastic cases. In the inset of Fig. 4 we plotted the average of the stretching rates (i.e., the first Lagrangian Lyapunov exponent of the flow λ_1^0) and the rescaled variance $\mu = T\langle\gamma_1^2\rangle$, for the three values of Wi that we considered. The decrease of the Lyapunov exponent (rescaled with the Newtonian value λ_1^N for comparison) gives a measure of the decrease in the chaoticity of the flow, due to the action of Polymers. On the other hand, we also observe a decrease in the rela-

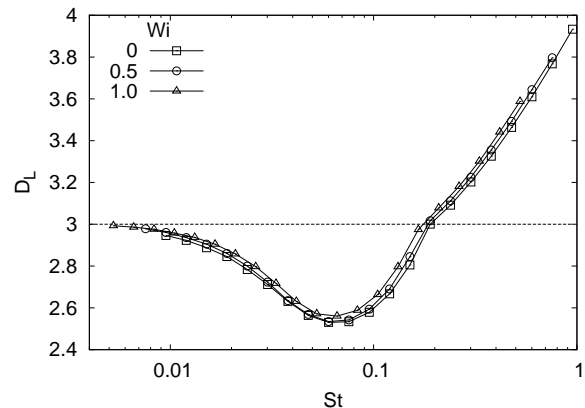
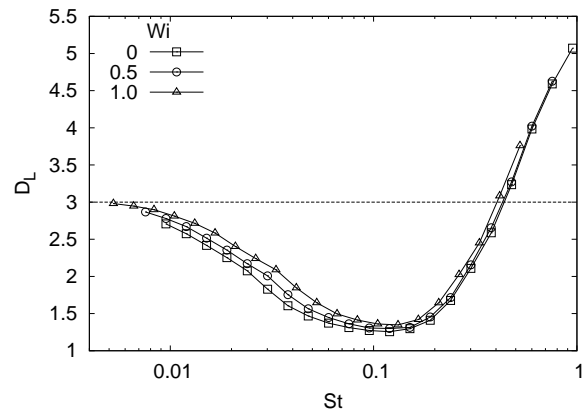


FIG. 5: Lyapunov dimension for light (upper panel) and heavy (lower panel) particles plotted as a function of $St = \tau_S \lambda_1^0$. Different lines correspond to the different Weissenberg numbers with symbols as in Fig. 2.

tive variance μ/Λ_1^0 , which implies that polymer feedback induces also a reduction of the fluctuations of stretching rates. Inspection of the main panel of Fig. 4, however, shows that fluctuations are not reduced uniformly. Indeed, the shape of $P(\gamma_1)$ changes when polymers are added. As is evident in Fig.4, elasticity has the effect of raising the right branch of the Cramér function, while the left one is comparatively less affected. Given the definition of $H(\gamma_1)$, this amounts to a relative suppression of positive fluctuations in the stretching rate: as one could expect, polymers have a larger (negative) feedback on events of larger stretching.

The effect of polymers on Lyapunov exponents and the Lagrangian nature of the latter suggests to introduce the dimensionless Stokes number defined as $St = \tau_S \lambda_1^0$ which depends on Wi by the dependence of λ_1^0 shown in Fig. 4. Figure 5 shows the Lyapunov dimension D_L for both heavy and light particles as a function of St . It is evident that, with respect to Fig. 2, the collapse of the curves at different Wi is improved. In particular, the minimum of the fractal dimension (which corresponds to maximum clustering) occurs almost for the same St number. Still, some differences are observable, in particular for small St in the case of light particles. This

can be understood by the following argument. Bubbles, at variance with heavy particles, have tendency to concentrate on filaments of high vorticity. Indeed, while the minimal dimension for heavy particles is about 2.5 (at $St \simeq 0.1$), for light particles at maximal clustering it becomes as small as 1.26. Vortex filaments correspond to quasi-one-dimensional regions of intense stretching, in the direction longitudinal to the vortex, which give major contributions to the right tail of the Cramér function. As shown in Fig. 4, the effects of polymers on the distribution of Lyapunov exponent is more evident in this region of strong fluctuations, where the distribution does not rescale with λ_1^0 . It is therefore not surprising that also the effects on clustering of light particles cannot be completely absorbed in the rescaling of τ_S with the mean stretching rate λ_1^0 .

As the fractal dimension is given by a combination of the Lyapunov exponents, in order to better understand the differences on light and heavy particles, in Fig.6 we show the first three Lyapunov exponents as a function of St . The first observation is that bubbles, at variance with heavy particles, exhibit negative values of λ_2 , consistently with the lower value of D_L and the tendency of light particles to concentrate towards vortex filaments.

The first Lyapunov exponent decreases with Wi for any value of St , thus indicating that the phenomenon of chaos reduction, already discussed for the case of Lagrangian tracers, is generic also for inertial particles. On the contrary, the second Lyapunov exponent shows a different behavior for light and heavy particles: it increases for the former but slightly decreases for the latter. Figure 6 shows that the effect of polymers is not a simple rescaling of the Lyapunov spectrum, which would trivially keep the dimension D_L unchanged. From this point of view, the almost perfect rescaling of the Lyapunov dimensions shown in Fig. 5 is quite surprising and arises as the result of compensations of different effects.

In conclusion, we investigated the clustering properties of inertial (heavy and light) particles in a turbulent viscoelastic fluid. The main effect of polymers on turbulent flows is to counteract small-scale fluctuations and to reduce its chaoticity. Quantitatively, this results in a decrease in the first Lyapunov exponent of the flow, which, in turn, affects clustering of inertial particles. The latter can be quantified by means of the fractal (Lyapunov) dimension of particle distributions. Although the effects of polymers on the particle Lyapunov exponents are complex and qualitatively different for light and heavy particles, the overall effect on fractal dimension is relatively

simple and can be rephrased in the rescaling of the characteristic time of the flow. Indeed, when particle inertia is parametrized by the Stokes number St defined with the Lyapunov time of the flow, one can approximately rescale the curves $D_L(St)$ at all Wi . In contrast, as polymers do not affect large scale properties of the flow, a parametrization of particle inertia based on integral time scales would not show a collapse of the curves $D_L(St)$ at different Wi . As a consequence, any prediction of par-

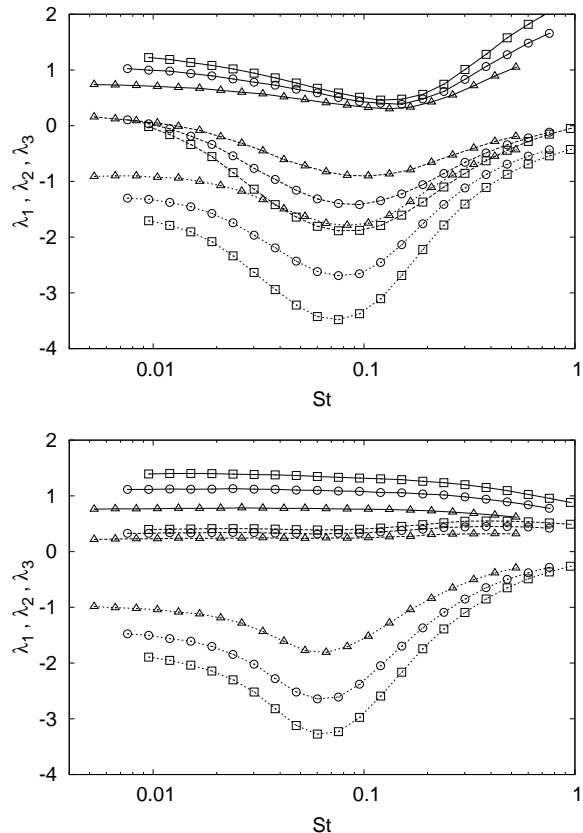


FIG. 6: The first three Lyapunov exponents for light ($\beta = 3$, upper panel) and heavy ($\beta = 0$, lower panel) particles, at different Wi . Continuous, dashed and dotted lines represent the first, second and third Lyapunov exponents, while symbols correspond to different Wi as in Fig. 2.

ticle clustering in turbulent polymeric solutions requires an accurate estimate of small scale stretching rates.

We acknowledge support from the the EU COST Action MP0806.

-
- [1] G. Falkovich, A. Fouxon, and M. Stepanov, *Nature* **419**, 151 (2002).
 - [2] A. Bracco, P. Chavanis, A. Provenzale, and E. Spiegel, *Phys. Fluids* **11**, 2280 (1999).
 - [3] K. Squires and J. Eaton, *Phys. Fluids A* **3**, 1169 (1991).
 - [4] M. Cencini, J. Bec, L. Biferale, B. G., C. A., A. Lanotte,

- S. Musacchio, and F. Toschi, *J. Turbul.* p. N36 (2006).
- [5] J. Bec, *J. Fluid Mech.* **528**, 255 (2005).
- [6] J. Warnatz, U. Maas, and R. Dibble, *Combustion: physical and chemical fundamentals, modeling and simulation, experiments, pollutant formation* (Springer Verlag, 2006).

- [7] D. Rouson and J. Eaton, *J. Fluid Mech.* **428**, 149 (2001).
- [8] F. Sbrizzai, V. Lavezzo, R. Verzicco, M. Campolo, and A. Soldati, *Chem. Eng. Sci.* **61**, 2843 (2006).
- [9] H. Barnes, *Rheology reviews* p. 1 (2003).
- [10] J. Lumley, *Annu. Rev. Fluid Mech.* **1**, 367 (1969).
- [11] A. Groisman and V. Steinberg, *Nature* **405**, 53 (2000).
- [12] G. Boffetta, A. Celani, and S. Musacchio, *Phys. Rev. Lett.* **91**, 34501 (2003).
- [13] A. M Crawford, N. Mordant, H. Xu, and E. Bodenschatz, *New J. Phys.* **10**, 123015 (2008).
- [14] A. Groisman and V. Steinberg, *Nature* **410**, 905 (2001).
- [15] E. Calzavarini, M. Kerscher, D. Lohse, and F. Toschi, *J. Fluid Mech* **607**, 13 (2008).
- [16] J. Bec, *Phys. Fluids* **15**, L81 (2003).
- [17] R. Sureshkumar and A. Beris, *J. Non-Newton. Fluid.* **60**, 53 (1995).
- [18] M. Maxey and J. Riley, *Phys. Fluids* **26**, 883 (1983).
- [19] R. Sureshkumar, A. Beris, and R. Handler, *Phys. Fluids* **9**, 743 (1997).
- [20] G. Boffetta, A. Celani, and A. Mazzino, *Phys. Rev. E* **71**, 036307 (2005).
- [21] S. Berti, A. Bistagnino, G. Boffetta, A. Celani, and S. Musacchio, *Phys. Rev. E* **77**, 055306 (2008).
- [22] O. H. R.B. Bird, R.C. Armstrong, *Dynamics of Polymeric Fluids*, vol. 2 (Wiley, New York, 1987).
- [23] J. Bec, L. Biferale, G. Boffetta, M. Cencini, S. Musacchio, and F. Toschi, *Phys. Fluids* **18**, 091702 (2006).
- [24] M. Cencini, F. Cecconi, and A. Vulpiani, *Chaos: from simple models to complex systems* (World Scientific Pub Co Inc, 2010).
- [25] T. Sauer and J. Yorke, *Ergodic Theory and Dynamical Systems* **17**, 941 (1997).
- [26] B. Hunt and V. Kaloshin, *Nonlinearity* **10**, 1031 (1997).
- [27] J. Bec, M. Cencini, and R. Hillerbrand, *Physica D* **226**, 11 (2007).
- [28] E. De Angelis, C. Casciola, R. Benzi, and R. Piva, *J. Fluid Mech.* **531**, 1 (2005).
- [29] P. Perlekar, D. Mitra, and R. Pandit, *Phys. Rev. Lett.* **97**, 264501 (2006).
- [30] G. Boffetta, A. Celani, and S. Musacchio, *Phys. Rev. Lett.* **91**, 34501 (2003).
- [31] E. Balkovsky, A. Fouxon, and V. Lebedev, *Phys. Rev. E* **64**, 056301 (2001).
- [32] E. Balkovsky, A. Fouxon, and V. Lebedev, *Phys. Rev. Lett.* **84**, 4765 (2000).